Removal of lead from aqueous solutions using cantaloupe peels as a biosorbent vs. cement kiln dust as an industrial by-product

Ahmed A. El-Refaey[a,*], Somaia G. Mohammad[b]

[a]*Department of Soil & Water Science, Faculty of Desert and Environmental Agriculture, Matrouh University, Matrouh, Egypt,*
email: ahmedelrefaey@alexu.edu.eg (A.A. El-Refaey)
[b]*Pesticide Residues and Environmental Pollution Department, Agriculture Research Center (ARC), Dokki, Giza, 12618, Egypt,*
email: sommohammad2015@gmail.com (S.G. Mohammad)

ABSTRACT

This study compared the removal of lead from aqueous solutions by cantaloupe peels (CP) as biosorbent against cement kiln dust (CKD) as an industrial byproduct. CP and CKD were characterized by pH, total carbon, nitrogen, and hydrogen content, thermo-gravimetric analysis (TGA), scanning electron microscopy (SEM), energy dispersive spectroscopy (EDX), Fourier transform infrared (FTIR), surface areas and pore volume to clarify the differences of physicochemical properties. CKD expressed a high affinity for removal of Pb^{2+} in all examine conditions, while CP was significantly affected, which reflects dissimilarity in the retention mechanisms defendant in CKD and those pursued by CP. The results were confirmed by changes in the FTIR and SEM images before and after sorption experiments. The experimental isotherms data were examined by Freundlich, Langmuir and Temkin isotherm equations. Langmuir isotherm model was more fitted to both sorbents with the highest correlation coefficient. The kinetic data were evaluated by fractional power, Elovich, pseudo-first order, and pseudo-second-order kinetic models. The pseudo-second-order kinetic model was found to adequately explain the kinetics and correlate with the experimental data well. The thermodynamic parameters revealed that the removal of Pb^{+2} by both CP and CKD at 298K–323 ± 2 K was a spontaneous and exothermic process. The results exposed that CP and CKD could be used as an efficient sorbent for lead removal from aqueous solution with privileges for CKD in all examine conditions.

Keywords: Lead removal; Cantaloupe peels; Biosorbent; Cement kiln dust; Isotherm; Kinetic; Thermodynamic

1. Introduction

Removal of heavy metals from contaminated environmental media gained great attention throughout recent years due to their classification as dangerous and carcinogenic and bio-accumulation through the organism's chain leading to chronic detrimental effects. Lead is one of the remarkable heavy metals used in many sectors and industries products. Due to its ductile and easily shaped such as cables, lead is used in batteries, petrol additives, chemical compounds, pigments, ceramics and glass productions [1]. Lead exposure remains to represent a serious threat to human health and to the environment. Lead is classified by the World Health Organization (WHO) as one of the hazardous and non-biodegradable heavy metals posing danger to human and other life forms [2].

There are many techniques for removing heavy metals from contaminated environment depending on the chemical, physical and biological methods. The most common treatment methods used for cleaning wastewater are adsorption, chemical precipitation, chemical oxidation, coagulation, electrodialysis, ultrafiltration and reverse osmosis. Adsorption process is still recognized as effectiveness and high-efficiency in heavy metals recovery from wastewater.

*Corresponding author.

Various materials are widely used as adsorbents such as activated carbon, zeolites, and clay minerals. Efficiency, low-cost, simplicity, and eco-friendly are important factors affecting the selection between them. Using non-conventional adsorbents such as agricultural waste and industrial by-product for the removal of toxic metals could be economic and potentially important choices in water reuse and scarcity scenarios [3,4].

Because of its low-cost and eco-friendly characteristics, biosorption technology has huge scope in wastewater treatment compared to other methods [5,6]. An enormous number of low-cost and easily available biosorbents could be used in the removal of hazardous wastes from aqueous solutions. Vegetable and fruit peels are common waste generated in the kitchen garbage and during industries processing. Its application as biosorbents may contribute to solving part of the problem of agricultural waste disposal [7,8]. Recent studies have been focused in their capacity to remove dyes [9,10], organic pollutants and pesticide [11–14], and heavy metals [15–20] from aqueous solutions. Cantaloupe (*Cucumis melo L.*) is one of the popular fruity vegetable grown in Egypt and used mainly as a dessert and refreshing fruit. Agricultural waste such as peel is a lignocellulose biomass-rich material and could be efficiently used as a low-cost biosorbent due to local availability and excellent adsorption capacity [5,7].

On the other hand, cement kiln dust (CKD) is a fine-grained solid substance created as a by-product material in the cement manufacturing process. CKD collected by bag-houses or electrostatic precipitators from cement kiln exhaust gases and estimated to 15–20% of cement clinker production [21]. CKD could be used in soil stabilization, waste solidification, cement additive, mine reclamation, agricultural soil amendment, sanitary landfill liner, wastewater treatment, pavement works, and concrete blocks, sludge stabilizers [22]. Furthermore, CKD could be used effectively in removing heavy metals ions from solutions due to its high content of alkali oxides, high surface area and excellent thermal resistance [3,22–24].

The purpose of this study is to investigate and evaluate lead removal by cantaloupe peels (CP) as an agricultural waste biosorbent compared to cement kiln dust (CKD) as an industrial by-product and hazardous solid waste. A comprehensive study of the adsorption procedure with various operating parameters such as initial lead concentration, initial pH, sorbent doses and contact time was conducted to evaluate the sorbents. Furthermore, lead sorption isotherm and kinetics of CP and CKD were evaluated in batch experiments.

2. Materials and methods

2.1. Characterization of CP and CKD

Cantaloupe fruits were collected from a local market, Cairo, Egypt. The Cantaloupe peel (CP) was separated, washed with distilled water and cut into small pieces and dried at 70°C for 48 h, then crushed and sieved using a 0.5-mm polypropylene sieve and stored in jars. CKD was obtained from El-Amerya of cementplants, Alexandria, Egypt. The pH of CP and CKD was measured in distilled water (1:2.5 H$_2$O). Total carbon, nitrogen and hydrogen content in CP and CKD were determined by CHNS analyzer (Elementar, Vario EL, Germany). The specific surface area of CP and CKD were determined by Brunauer–Emmett–Teller (BET) equation from N$_2$ isotherms at 77 K under relative pressures (P/P_o) ranged from 0.02 to 0.3 using a gas sorption analyzer (Beckman Coulter SA(TM) 3100 surface area and pore size analyzer). In addition, total pore volume was estimated from N$_2$ adsorption at $P/P_o = 0.99$ [25].

Thermo gravimetric analysis (TGA) of CP and CKD were conducted in the Thermo gravimetric analyzer (Pyris Diamond TG/DTA, Perkin Elmer, Singapore) in nitrogen atmosphere (150 ml min^{-1}) in platinum crucibles with temperature ranged from 30°C to 1000°C and heating rate 20°C min^{-1}.

In order to Identify the functional groups composition for CP and CKD, Fourier transform-infrared (FTIR) spectra at the range 400–4,000 cm^{-1} using KBr pellet method was obtained by a Fourier transforms infrared spectrometer (model FT/IR-5300, JASCO Corporation, Japan).

The surface morphology of CP and CKD was examined by Scanning electron microscopy (SEM) using a Jeol JSM-5300 scanning electron microscope and was operated between 15 and 20 kV. Before the SEM examines, samples were gold-coated in a sputter coating unit (JFC-1100 E). The micrographs were recorded at various magnification scales using photographic techniques to characterize the morphology of CP and CKD. Also, in order to clarify the nature and element contents of CP and CKD, the analyses of energy dispersive spectroscopy (EDX) were used. For EDX, the element percentage was an average of three examined field. FTIR, SEM and EDX analyses were carried out before and after sorption experiments.

2.2. Batch experiments

Lead sorption isotherms and kinetics on CP and CKD were evaluated by batch experiments. Solutions of lead concentrations prepared by Pb(NO$_3$)$_2$ that obtained from Merck (Germany). A 0.30 g of the adsorbent was placed in 250 ml flask with 25 ml of 20 mg Pb/L) at ambient room temperature in a rotary shaker at 200 rpm. A series of batch studies were carried out to examine the effect of adsorption time, pH, adsorbent doses, initial concentration on lead sorption capacity of CP and CKD. The optimal pH values in the tested solution were obtained using 1 M NaOH or 0.5 M HCl. All of the experiments were carried out in duplicates. Pb^{2+} concentrations were measured in filtrate by using Agilent 4200 Microwave Plasma-Atomic Emission Spectrometer (MP–AES).

The sorption capacity (q_e) was determined by:

$$q_e = \frac{(C_o - C_e)V}{m} \tag{1}$$

where C_o and C_e are the initial and the equilibrium concentrations in mg/L, respectively, V is the volume of solution (ml) and m is the amount of adsorbent used (g). The removal efficiency of Pb^{2+} from solution was calculated by:

$$\text{Removal efficiency } (\%) = \frac{(C_o - C_t)}{C_o} \times 100 \tag{2}$$

2.3. Sorption isotherm studies

Sorption data were fitted to the following known adsorption isotherm models in order to determine the adsorption parameters [11]:

Freundlich

$$q_e = K_F C_e^{1/n} \tag{3}$$

Langmuir

$$q_e = q_{max}(K_L C_e / 1 + K_L C_e) \tag{4}$$

Temkin

$$\theta = RT / \Delta Q \ln K_o C_e \tag{5}$$

where q_e (mg g^{-1}) is Pb^{2+} adsorbed per gram of adsorbent, C_e (mg L^{-1}) is equilibrium Pb^{2+} concentration in solution, K_F is a constant related to adsorption capacity of the adsorbent (mg$^{1-(1/n)}$ L$^{1/n}$g^{-1}), n is a constant, q_{max} (mg g^{-1}) is the maximum adsorption capacity of the adsorbent, K_L (L mg^{-1}) is Langmuir constant related to the free energy of adsorption, θ is fractional coverage, R is the universal gas constant (kJ mol^{-1} K^{-1}), T is the temperature (K), ΔQ is ($-\Delta H$) variation of adsorption energy (kJ mol^{-1}), and K_o is Temkin constant (L mg^{-1}).

2.4. Kinetics studies

Four kinetic models were applied to the sorption data to understand the effect of time on the sorption process. The four equations are fractional power, Elovich, pseudo-first-order and pseudo-second-order models. The following known adsorption kinetic models [3]:

Fractional power:

$$q_t = a\, t^b \tag{6}$$

Or by its linear form:

$$\ln q_t = \ln a + b \ln t \tag{7}$$

where q_t is the amount of Pb^{2+} sorbed by CP and CKD at a time t, while a and b are constants with $b < 1$. ab is specific sorption rate at unit time.

The semi-empirical equation Elovich:

$$\frac{dq_t}{dt} = \alpha \exp\left(-\beta q_t\right) \tag{8}$$

or in the integrated form

$$q_t = \frac{1}{\beta}\ln(\alpha\beta) + \frac{1}{\beta}\ln t \tag{9}$$

where α is the initial adsorption rate (mg g^{-1} min^{-1}), and the parameter β is related to the extent of surface coverage and activation energy for chemisorption (g mg^{-1}).

The pseudo-first-order model:

$$\log\left(q_e - q_t\right) = \log q_e - k_1 t / 2.303 \tag{10}$$

The pseudo-second order model:

$$\frac{t}{q_t} = \frac{1}{k_2 q_e^2} + \frac{t}{q_e} \tag{11}$$

where k_1 is the pseudo-first-order rate constant (min^{-1}), k_2 (g mg^{-1} min^{-1}) is the pseudo-second-order rate constant and q_e (mg g^{-1}) is the adsorption capacity at equilibrium and q_t (mg g^{-1}) is the amount of metal adsorbed at a given time t.

3. Results and discussion

3.1. Characteristics of CP and CKD

Characterization of CP and CKD are recorded in Table 1. The pH for CP was acidic (5.24) but CKD was alkaline (10.20). For element contents, CP was higher in total carbon, nitrogen and hydrogen content compared to CKD excluding sulfur content, it was higher in CKD (0.84%) than CP (0.18%). Surface area and pore volume are important properties that play major roles in stability and purification. The nitrogen BET method is a common technique for determining the surface area for its simplicity and reasonable forecasts with rigorous limitations [26]. Results indicated that the specific surface area of CKD was higher than CP 20.98 m^2/g and 0.33 m^2/g, respectively (Table 1). Total pore volume for CKD (37.30 mm^3 g^{-1}) was higher than CP (13.9 mm^3 g^{-1}). Properties of CKD depend upon the raw materials, plant configuration, and the preprocessing type [22].

3.2. TGA- analysis

Thermogravimetric analysis (TGA) represents the thermal decomposition with increasing temperature. TGA of CP and CKD illustrated in Fig. 1. The initial weight loss for CP is approximately 17% at 200°C and can be accounted to moisture content and some volatile organic components. The second weight loss stage is extended to 336°C corresponded to degradation of hemicelluloses. Cellulose degradation occurred after hemicelluloses degradation stage when temperature ranges between 336–528°C where the sample loss about 13% of its weight. Another 6% of weight loss occurred at 850°C attributed to decomposition of lignin content (Fig. 1). TGA analysis showed that the hemicellulose (36%) is the easily degradable ingredient followed by the cellulose (13%) compared to lignin; considered as the most stable and smallest weight loss (6%) compound. Similar results obtained by Yang et al. [27], Pathak et al. [28] and Basu et al. [29]. On the other hand, CKD is known as thermal resistance material due to its composition of calcined materials and combustion by-products [3, 22,30,31]. TGA analysis for CKD confirmed the thermal stability of CKD (Fig. 1). The dehydration of CKD reached 7% weight loss in the first stage due to the loss of adsorbed water molecules. With increasing the temperature from 530°C to 700°C, CKD lost about 18% of its weight attributed dehydration of calcium hydroxide due to the calcination of calcium carbonate and its conversion into calcium oxide [32,33].

3.3. FTIR analysis

FTIR technique is a successful and accurate analysis device to recognize the features of functional groups, change

Table 1
Characteristics of cantaloupe peel (CP) and cement kiln dust (CKD)

	pH	%				Surface area m^2 g^{-1}	Total pore volume mm^3 g^{-1}
		C	H	N	S		
CP	5.24	36.02	4.31	2.04	0.18	4.61	0.33
CKD	10.20	6.35	0.19	Nil	0.84	20.98	37.30
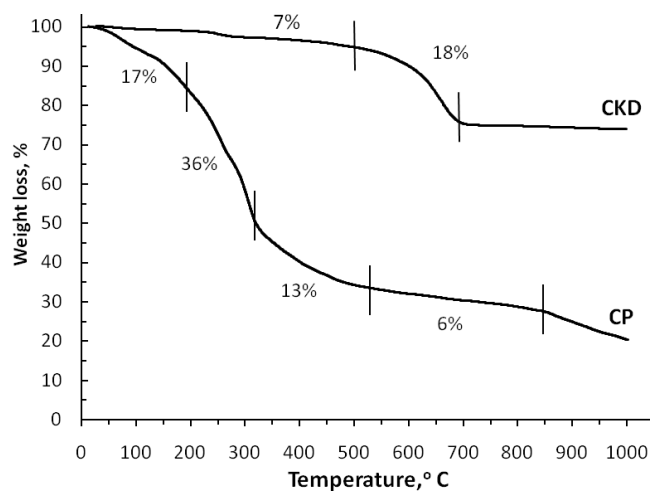
Fig. 1. Thermo gravimetric analysis (TGA) of cantaloupe peels (CP) and cement kiln dust (CKD) at different temperatures, numbers on curves indicated weight losses percent per each stage.

in chemical compositions, interface and hence properties [34,35]. The FTIR spectra of the CP and CKD before and after the sorption of Pb ions from aqueous solutions are presented in Fig. 2. The FTIR spectra of CP showed the bands located at 3423.94 cm^{-1} confirmed the presence of O–H (hydroxyl) and N-H of amines while bands at 2927.41 cm^{-1} indicates the stretching vibrations of –CH$_3$ or –CH$_2$ groups [11,36]. Peak positions at 1733.69 cm^{-1} and 1628.59 cm^{-1} accounted for C=O stretching of esters and carboxylate ions. The stretching peak at 1428.94 revealed C-H deformation of aldehydes and alkanes. The peaks at 1251.58 cm^{-1} and 1058.73 cm^{-1} indicate the presence of C-O stretching vibrations in alcohols, phenols, acids, ethers, or esters [29,37]. Peaks position at 879.38 cm^{-1} and 599.75 cm^{-1} are attributed to amine groups and C-H bend alkenes (tri-substituted) [11,36].

On the other hand, the FTIR spectrum of CKD shows peak positions at 3437.49, presence of O–H (hydroxyl) could be also detected at 3437.49 and 1796.37 cm^{-1} while the bands at 1037.52 and 711.60 reflect the existence of the silicate. The band at 2515 cm^{-1} is attributed to CC stretching vibration in alkyne group. However, the vibration related to K–O is observed at wave number of 611.32 cm^{-1} [31,33,38,39]. Slight shifts were observed in FTIR bands of studied sorbents after the sorption reaction with lead ions which confirm the attachment of lead ions on CP and CKD (Fig. 2).

3.4. SEM and EDX analysis

Scanning electron microscopy (SEM) is among the widely used tools to investigate the surface characteriza-
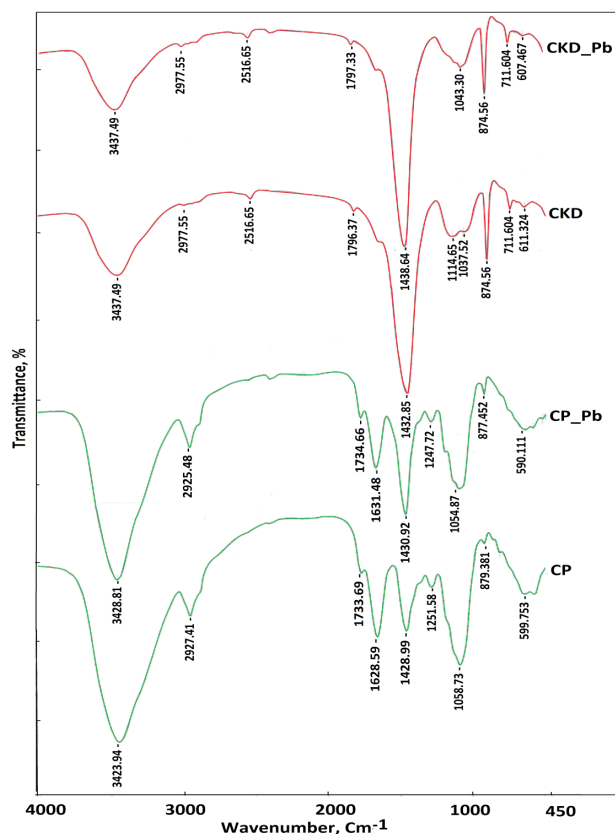
Fig. 2. FTIR spectra of cantaloupe peels (CP) and cement kiln dust (CKD) before and after the sorption of Pb^{+2} from aqueous solutions.

tion specially lignocelluloses [40]. The textural and morphological structure examination of CP and CKD were analyzed by SEM before and after Pb^{+2} adsorption experiment (Fig. 3). It was observed that the surfaces of CP is rough and uneven and have some pores. These pores can play important role in adsorption of soluble and insoluble pollutants with great adsorption capacity. On other hand, the SEM examination of CKD showed that CKD has the finest particle sizes as well as the highest surface areas. The changes between before and after adsorption observed in porous structure of CKD were more than that observed in CP. A minor softening was observed on edges of the pores of CP samples after the reaction with Pb^{+2}, while CKD particles were covered by precipitates or complexes formation. This may denote various mechanisms for Pb^{+2} removals. However, the SEM technique has also some limitations and incapability to
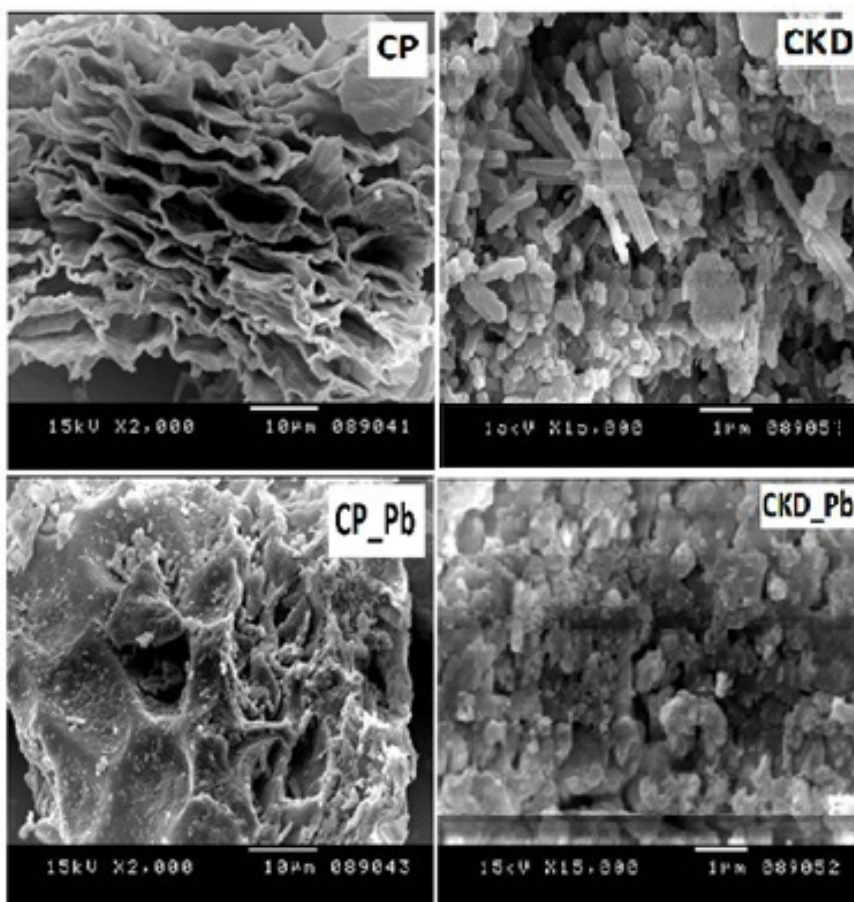
Fig. 3. SEM micrographs of cantaloupe peels (CP) and cement kiln dust (CKD) before and after the removal reactions of Pb^{+2} from aqueous solutions.

detect trace elements in a substance unless it is equipped with an energy-dispersive spectroscopy (EDX). EDX can indicate the elemental composition with acceptable precision and accuracy. The EDX analysis of CP shows various element compositions (Fig. 4). The spectrum of EDX indicated peaks of Mg (1.8%), Al (1.7%), Si (2.0%), P (11.4%), S (2.7%), Cl (14.4%), K (40.0%), Ca (18.5%), Cu (3.7%) and Zn (1.8%). Compared to the spectrum of EDX after adsorption experiment, it was observed that peaks of K and Mg were reduced to 5.9% and 1.2%, respectively accomplished with the presence of Pb (5.1%). This reduction could suggest that ion exchange involved in the removal of lead by CP from aqueous solution [29]. The EDX analysis of CKD shows the presence of high content of calcium (Fig. 4). For CKD, EDX analysis obviously indicated the high calcium contents (80.5%). The EDX spectrum of CKD showed peaks of Mg (0.4%), Al (0.7%), Si (3.8%), S (2.1%), Cl (5.3%), K (3.5%), Ca (80.5%), Fe (1.9%), Cu (1.3%) and Zn (0.8%). The EDX analysis of CKD after the lead removal experiment also shows the reduction of K and Mg peaks to 0.7% and 0–0.1% respectively accomplished with the presence of Pb (0.8%) (Fig. 4). Moreover, the EDX spectrum of CKD after the lead removal experiment showed an increase in Ca peaks (88.5%) in the surface of inspected samples that may

be suggested more mechanism than ion exchange is involved in lead removal by CKD.

3.5. Lead removal by CP and CKD

Removal of Pb^{+2} from aqueous solution by CP and CKD with time, adsorbent dose, initial concentration and initial pH is presented in Fig. 5. Removal of Pb^{+2} by CP increased to reach 80.2% after one hour and continues to increase to 92.2% after 9 h then tended to decrease with time to 34.6% after 48 h (Fig. 5a). This shifting in removing trend to decrease could be result of the decomposition of CP material. Saleh et al. [36] and Adelagun et al. [41] obtained similar trend with agricultural residual and unmodified biosorbents accomplish with increasing of dissolved organic carbon (DOC) released from sorbent materials. On other hand, CKD showed a strong affinity of removing Pb^{+2} (more than 99%) after 5 min of the removal reaction and showed stability and did not affect with increasing of reaction time (Fig. 5a). The strong affinity of removing Pb^{+2} by CKD (more than 99%) was also observed with increasing mass dose (Fig. 5b), the initial concentration (Fig. 5c) and initial pH (Fig. 5d) and did not affect of with changing of their rates. This high affinity could be explained by high calcium carbonate and calcium oxide contents, surface area, oxide con-
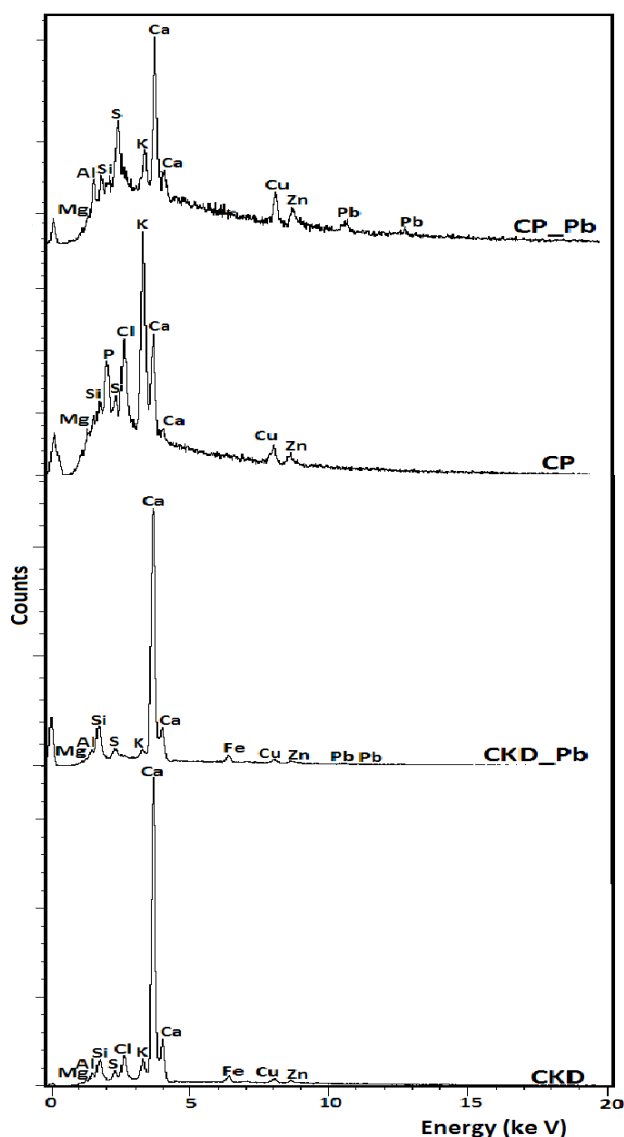
Fig. 4. EDX spectrum of cantaloupe peels (CP) and cement kiln dust (CKD) before and after the removal reactions of Pb^{+2} ions from aqueous solutions.

tent and reducing metal solubility which enhanced sorption and/or precipitation [3,24,30,42,43]. On the other side, CP showed increasing in removal percentage from 80.70 to 94.92 with increasing of mass load from 0.01 g to 0.6 g (Fig. 5b) and decreased in removal percent from 95.00 to 81.03 along with increasing the initial concentration from 5 to 100 mg L^{-1} (Fig. 5c). As the initial pH increased, the lead removal percentage by CP reached its maximum value (95.4%) at pH 4.0 (Fig. 5d). However, Basu et al. [29] and Abbaszadeh et al. [44] reported a similar pattern of lead adsorption, but reaching an optimum value at pH value equal to 5.0 for cucumber and papaya peels.

3.6. Sorption isotherms

The lead sorption isotherms of CP and CKD were evaluated by Freundlich, Langmuir and Temkin (Table 2). The

lead sorption by CP and CKD was fitted to the Langmuir and Freundlich isotherm equations, respectively (Figs. 5e and 5d). The sorption curve was more closely to Langmuir equation, compared by R^2 values to distinguish how to estimate model close to experimental data. The R^2 for CP was founded to be 0.956 and 0.995 for Freundlich and Langmuir models, respectively, while the corresponding values for CKD were 0.915 and 0.939, respectively, and significantly at level P = 0.01 (based on Pearson's error). The maximum sorption capacity of CKD for Pb^{2+} (42.37 mg g^{-1}) was significantly higher than CP (22.27 mg g^{-1}) (Table 2).

3.7. Kinetics studies

The experimental kinetic data were fitted to fractional power, Elovich, pseudo-first, and pseudo-second-order equation. The kinetic parameters are shown in Table 3. As compared by value of the determination coefficient (R^2), the pseudo-second-order model is the highest value ($R^2 > 0.99$), fitted to the adsorption kinetics of Pb^{+2} onto CP and CKD and significantly at level $P = 0.01$ based on Pearson's Error (Fig. 6). Furthermore, experimental q_e values are very close to those calculated for the pseudo second-order kinetic model with high value for CKD than CP. That may support the suggestion of the adsorption process is most likely chemisorptions [45,46]. According to metal ions adsorption theory, removal of Pb^{+2} could be explained by different mechanism: electrostatic interaction with negatively charged surface functional groups (cation exchange), specific metal–ligand complexation relating to surface functional groups of sorbents, and/or physical sorption controlled by surface area and porosity [3,36,46]. For CP, ion exchange may play important role in removal of lead, indicating by the reduction of K and Mg accomplished with increasing of Pb percent in the spectrum of EDX after adsorption experiment (Fig. 4). Similar results reported by Basu et al. [29]. On the other hand, CKD results confirmed that different mechanisms control the removal process, supported by increase in Ca peaks in EDX spectrum and agglomerates form in SEM images after adsorption of CKD (Fig. 5). The calcium carbonate, calcium oxide contents, as well as high alkalinity attributed to removal of Pb^{2+} by CKD mechanisms and enhanced sorption (electrostatic ion exchange and complex reactions) and/or precipitation [3,24,43].

3.8. Thermodynamic studies

The thermodynamic parameters, the Gibbs free energy ($\Delta G°$), the enthalpy change ($\Delta H°$) and the entropy change ($\Delta S°$), for the adsorption process of Pb^{2+} by CP and CKD from aqueous solutions in the temperature range of 298K–323±2 K were estimated using the following equations [19,47]:

$$\Delta G° = -RT \ln K_c \tag{12}$$

$$\Delta G° = \Delta H° - T \Delta S° \tag{13}$$

where R is gas constant (8.314 J/mol K), K_c is the equilibrium constant and T is the absolute temperature (K). The K_c value is determined using Eq. (14):

$$K_c = \frac{q_e}{C_e} \tag{14}$$
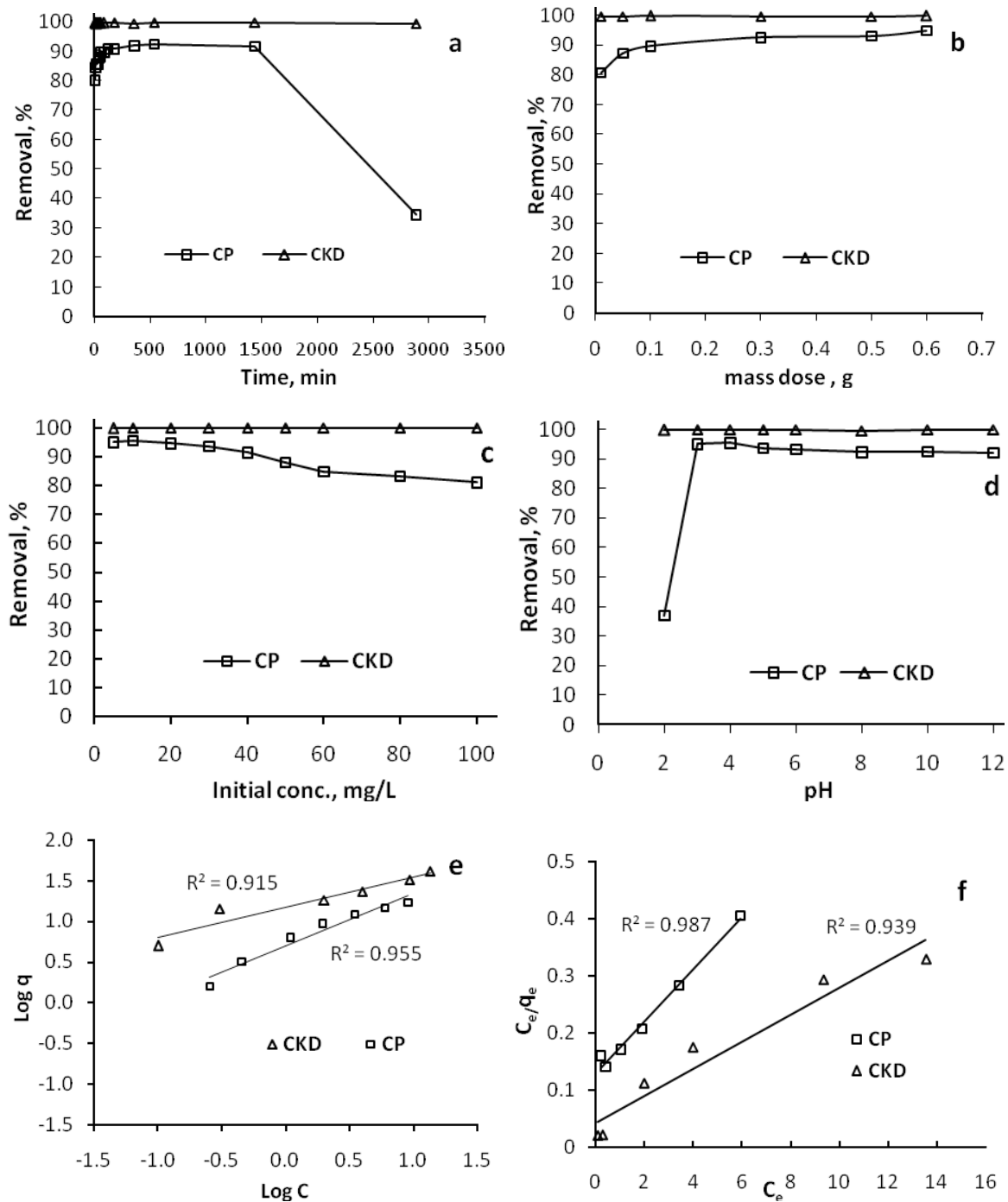
Fig. 5. Lead removal by cantaloupe peels (CP) and cement kiln dust (CKD). Removal percent with (a) time (min), (b) mass dose (gm), (C) at different initial lead concentrations and (d) with at different pH, (e) Lead adsorption isotherm regression using Freundlich equation and (f) Lead adsorption isotherm regression using the Langmuir equation; ** significance ($p<0.05$, based on Pearson's Error).

where q_e and C_e are the equilibrium concentration of metal ions on adsorbent (mg/g) and in the solution (mg/L), respectively. The well-known van't Hoff equation is obtained by substituting Eq. (13) into Eq. (15).

$$\ln K_c = -\frac{\Delta G^o}{RT} = -\frac{\Delta H^o}{RT} + \frac{\Delta S^o}{R} \qquad (15)$$

The calculated values of $\Delta G°$, $\Delta H°$, and $\Delta S°$ are given in Table 4. The negative $\Delta G°$ values indicate that the process is thermodynamically feasible, spontaneous and corresponding to a chemical process and virtually complete under just any reasonable set of conditions for the removal of Pb^{2+} by CP and CKD. Besides, the decrease in $\Delta G°$ values with increase in the temperature shows a decrease in feasibil-

Table 2
Adsorption isotherm parameters of Pb(II) unto CP and CKD

	Freundlich			Langmuir			Temkin		
	K_F mg$^{1-(1/n)}$ L$^{1/n}$g^{-1}	$1/n$	R^2	q_m mg g^{-1}	K_L L mg^{-1}	R^2	A L g^{-1}	B	R^2
CP	4.990	0.645	0.956	22.27	0.346	0.987	6.253	1.251	0.701
CKD	1.172	0.367	0.915	42.37	0.546	0.939	19.640	6.253	0.887

Table 3
Kinetic parameters for lead sorption by CP and CKD

	Fractional power			Elovich			Pseudo-first-order			Pseudo-second-order		
	a	b	R^2	α	β	R^2	q_e	k_1	R^2	q_e	k_2	R^2
CP	1.610	0.0002	0.026	2.86×10^8	3.943	0.790	1.201	0.0057	0.832	6.531	0.036	0.996
CKD	6.630	0.0431	0.812	2.69×10^{43}	833.33	0.026	3.266	0.001	0.924	6.636	0.794	0.999

Table 4
Thermodynamic parameters of Pb^{2+} removal by CP and CKD from aqueous solutions in the temperature range of 298K to 323±2K

	$\Delta G°$, kJ/mol			$\Delta S°$	$\Delta H°$
	298K	308K	323K	J/mol K	kJ/mol
CP	–15.35	–15.87	–16.64	–51.59	–22.10
CKD	–7.33	–7.58	–7.95	–24.67	–19.24

$\Delta G°$ – Gibbs free energy; $\Delta H°$ – enthalpy; $\Delta S°$ – entropy
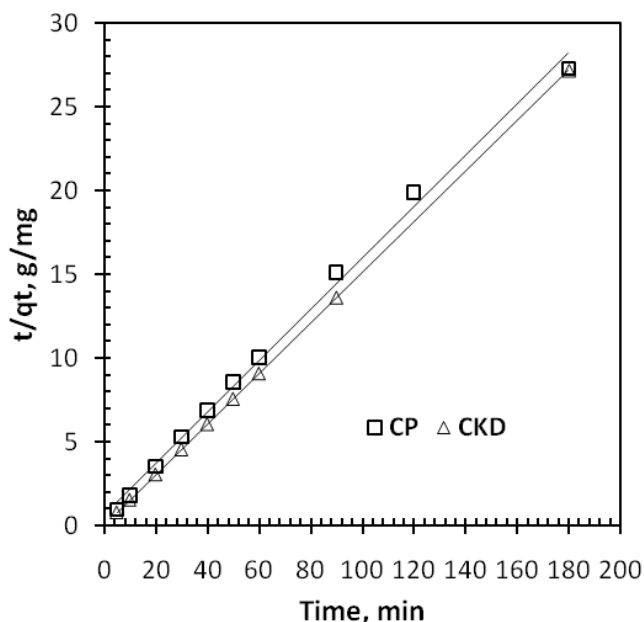
Fig. 6. Pseudo-second-order plots for Pb^{+2} removal kinetics by CP and CKD.

4. Conclusions

This study investigates and compares the removal of Pb^{2+} by CP and CKD. The results indicate the strong potential of CKD for removing Pb^{2+} from aqueous solutions in different circumstances (adsorption time, pH, adsorbent dose, initial concentration) in comparison to CP. The high efficiency of CKD could be explained by its high lime content, surface area, oxides content, and reducing metal solubility owed to enhanced sorption and/or precipitation. CP showed remarkable behaves in the removal of Pb^{2+} closed to CKD, but tend to decrease with time as a result of decomposition of CP and release of dissolved organic carbon. Time, pH, adsorbent dose and initial concentration, independence of Pb^{2+} removal by CKD may reflect differences in retention mechanisms defendant in CKD and those pursued by CP and this was confirmed by EDX results. The Langmuir isotherm model provided the best fitting to describe the lead sorption isotherm on CP and CKD. The pseudo-second-order kinetic model fits very well with the dynamic behavior for the removal of Pb^{2+} by CP and CKD. The thermodynamic studies showed the feasibility, spontaneous and exothermic nature of the sorption of Pb^{2+} onto CP and CKD in the temperature range of 298K to 323±2 K.

ity of sorption at higher temperatures. The negative value of $\Delta H°$ pointed out that the nature of adsorption process is exothermic. The negative $\Delta S°$ value echoes a decrease in the randomness at the solid/solution interface during the removal process of Pb(II) ions onto CP and CKD.

References

[1] B. Liu, W. Chen, X. Peng, Q. Cao, Q. Wang, D. Wang, X. Meng, G. Yu, Biosorption of lead from aqueous solutions by ion-imprinted tetraethylenepentamine modified chitosan beads, Int. J. Biol. Macromol., 86 (2016) 562–569.

[2] World Health Organization (WHO), Exposure to Lead: A Major Public Health Concern,WHO (2010), Geneva, Switzerland, http://www.who.int/ipcs/features/lead.pdf (accessed 1 August 2018).

[3] A.A. El-Refaey, Comparative performance of cement kiln dust and activated carbon in removal of cadmium from aqueous solutions, Water Sci. Technol., 73 (2016) 1691–1699.

[4] T. Ahmad, M. Danish, Prospects of banana waste utilization in wastewater treatment: A review, J. Environ. Manage., 206 (2018) 330–348.

[5] C. Djelloul, O. Hamdaoui, Removal of cationic dye from aqueous solution using melon peel as nonconventional low-cost sorbent, Desal. Water Treat., 52 (2014) 7701–7710.

[6] I.S. Bădescu, D. Bulgariu, I. Ahmad, L. Bulgariu, Valorisation possibilities of exhausted biosorbents loaded with metal ions – A review, J. Environ. Manage., 224 (2018) 288–297.

[7] A. Bhatnagar, M. Sillanpää, A. Witek-Krowiak, Agricultural waste peels as versatile biomass for water purification – A review, Chem. Eng. J., 270 (2015) 244–271.

[8] M. Ibrahim, A. Siddique, L. Verma, J. Singh, J.R. Koduru, Adsorptive removal of fluoride from aqueous solution by biogenic iron permeated activated carbon derived from sweet lime waste, Acta Chim. Slov., 66 (2019) 123–136.

[9] L.Y. Lee, S. Gan, Y.S. M. Tan, S.S. Lim, X.J. Lee, Y.F. Lam, Effective removal of Acid Blue 113 dye using overripe Cucumis sativus peel as an eco-friendly biosorbent from agricultural residue, J. Clean. Prod., 113 (2016) 194–203.

[10] L.B.L. Lim, N. Priyantha, D.T.B. Tennakoon, H.I. Chieng, M.K. Dahri, M. Suklueng, Breadnut peel as a highly effective low-cost biosorbent for methylene blue: Equilibrium, thermodynamic and kinetic studies, Arab J. Chem., 10 (2017) S3216–S3228.

[11] S.G. Mohammad, S.M. Ahmed, A.F. Badawi, A comparative adsorption study with different agricultural waste adsorbents for removal of oxamyl pesticide, Desal. Water Treat., 55 (2014) 2109–2120.

[12] R. Rojas, J. Morillo, J. Usero, E. Vanderlinden, H.E. Bakouri, Adsorption study of low-cost and locally available organic substances and a soil to remove pesticides from aqueous solutions, J. Hydrol., 520 (2015) 461–472.

[13] L.A. Romero-Canoa, L.V. Gonzalez-Gutierreza, L.A. Baldenegro-Perezb, Biosorbents prepared from orange peels using instant controlled pressure drop for Cu(II) and phenol removal, Ind. Crops Prod., 84 (2016) 344–349.

[14] L.P. Lingamdinne, J. Choi, J. Yang, Y. Chang, J.R. Koduru, J. Singh, Adsorptive removal of selected anionic and cationic dyes by using graphitic carbon material prepared from edible sugar: a study of kinetics and isotherms, Acta Chim. Slov., 65 (2018) 599–610.

[15] S. Ben-Ali, I. Jaouali, S. Souissi-Najar, A. Ouederni, Characterization and adsorption capacity of raw pomegranate peel biosorbent for copper removal, J. Clean. Prod., 142 (2017) 3809–3821.

[16] M. Ngabura, S.A. Hussaina, W.A. Ghania, M.S. Jamib, Y.P. Tan, Utilization of renewable durian peels for biosorption of zinc from wastewater, J. Environ. Chem. Eng., 6 (2018) 2528–2539.

[17] N. Saranya, A. Abhishek , V. Sivasubramanian, N. Selvaraju, Hexavalent chromium removal from simulated and real effluents using artocarpus heterophyllus peel biosorbent - Batch and continuous studies, J. Mol. Liq., 265 (2018) 779–790.

[18] L.P. Lingamdinne, Y. Chang, J. Yang, J. Singh, E. Choi, M. Shiratani, J.R. Koduru, P. Attri, Biogenic reductive preparation of magnetic inverse spinel iron oxide nanoparticles for the adsorption removal of heavy metals, Chem. Eng. J., 307 (2017) 74–84.

[19] L.P. Lingamdinne, J. Yang, Y. Chang, J.R. Koduru, Low-cost magnetized Lonicera japonica flower biomass for the sorption removal of heavy metals, Hydrometallurgy, 165 (2016) 81–89.

[20] L.P. Lingamdinne, J.R. Koduru, R.K. Jyothi, Y. Chang, J. Yang, Factors affect on bioremediation of Co(II) and Pb(II) onto Lonicera japonica flowers powder, Desal. Water Treat., 57 (2016) 13066–13080.

[21] United States Environmental Protection Agency (USEPA), 2016, Cement Kiln Dust Wastes, https://archive.epa.gov/epawaste/nonhaz/industrial/special/web/html/index-2.html (accessed 1 August 2018).

[22] M.K. Rahman, O.S. Rehman, B. Al-Amoudi, Literature review on cement kiln dust usage in soil and waste stabilization and experimental investigation, IJSER., 7 (2011) 77–87.

[23] W.M. Salem, W.F. Sayed, S.A. Halawy, R.B. Elamary, Physicochemical and microbiological characterization of cement kiln dust for potential reuse in wastewater treatment, Ecotox. Environ. Safe, 119 (2015) 155–161.

[24] A.A. El-Refaey, Investigation of copper removal from aqueous solution by cement kiln dust as industrial by-product, Alexandria Sci. Exch. J., 38 (2017) 149–158.

[25] M. Naderi, Surface area: Brunauer–Emmett–Teller (BET), In: Progress in Filtration and Separation (S. Tarleton, ed.), Academic Press, London, UK, 2015, 585–608.

[26] B.S. Girgis, A.M. Soliman, N.A. Fathy, Development of micro-mesoporous carbons from several seed hulls under varying conditions of activation, Micropor. Mesopor. Mater., 142 (2011) 518–525.

[27] H. Yang, R. Yan, H. Chen, D.H. Lee, C. Zheng, Characteristics of hemicellulose, cellulose and lignin pyrolysis, Fuel, 86 (2007) 1781–1788.

[28] P.D. Pathak, A.M. Sachin, D.K. Bhaskar, Characterizing fruit and vegetable peels as bioadsorbents, Current Sci., 110 (2016) 2114–2123.

[29] M. Basu, A.K. Guha, L. Ray, Adsorption of lead on cucumber peel, J. Clean. Prod., 151 (2017) 603–615.

[30] N.G. Zaki, I.A. Khattab, N.M. Abd El-Monem, Removal of some heavy metals by CKD leachate, J. Hazard. Mater., 147 (2007) 21–27.

[31] A. Salem, H. Afshin, H. Behsaz, Removal of lead by using Raschig rings manufactured with mixture of cement kiln dust, zeolite and bentonite, J. Hazard. Mater., 223–224 (2012) 13–23.

[32] V.S. Ramachandran, J.J. Beaudoin, Handbook of Thermal Analysis of Construction Materials. 1st Ed., William Andrew, New York, 2003.

[33] M.E. Saraya, M.E. Aboul-Fetouh, Utilization from cement kiln dust in removal of acid dyes, Am. J. Environ. Sci., 8 (2012) 16–24.

[34] V.O. Arief, K. Trilestari, J. Sunarso, N. Indraswati, S. Ismadji, Review recent progress on biosorption of heavy metals from liquids using low cost biosorbents: Characterization, biosorption parameters and mechanism studies, Clean, 36 (2008) 937–962.

[35] K. Karimi, M.J. Taherzadeh, A critical review of analytical methods in pretreatment of lignocelluloses: Composition, imaging, and crystallinity, Bioresour. Technol., 200 (2016) 1008–1018.

[36] M.E. Saleh, A.A. El-Refaey, A.H. Mahmoud, Effectiveness of sunflower seed husk biochar for removing copper ions from wastewater: a comparative study, Soil Water Res., 11 (2016) 53–63.

[37] W. Tongpoothorn, M. Sriuttha, P. Homchan, S. Chanthai, C. Ruangviriyachai, Preparation of activated carbon derived from Jatropha curcas fruit shell by simple thermo-chemical activation and characterization of their physico-chemical properties, Chem. Eng. Res. Des., 89 (2011) 335–340.

[38] M.A. Al-Ghouti, M.A.M. Khraisheh, S.J. Allen, M.N. Ahmad, The removal of dyes from textile wastewater: a study of the physical characteristics and adsorption mechanisms of diatomaceous earth, J. Environ. Manage., 69 (2003) 229–238.

[39] A. Salem, E. Velayi, Application of hydroxyapatite and cement kiln dust mixture in adsorption of lead ions from aqueous solution, Ind. Eng. Chem. Res., 18 (2012) 1216–1222.

[40] H. Amiri, K. Karimi, Improvement of acetone, butanol, and ethanol production from woody biomass by using organosolv pretreatment, Bioprocess. Biosyst. Eng., 38 (2015) 1959–1972.

[41] R.O. Adelagun, E.P. Berezi, A.U. Itodo, O.J. Oko, E.A. Kamba, C. Andrew, H.A. Bello, Adsorption of Pb^{2+} from aqueous solution by modified melon (Citrullus lanatus) seed husk, Chem. Mater. Res., 6 (2014) 113–121.

[42] A.L.Mackie, M.E. Walsh, Bench-scale study of active mine water treatment using cement kiln dust (CKD) as a neutralization agent, Water Res., 46 (2012) 327–334.

[43] M. El Zayat, S. Elagroudy, S. El Haggar, Equilibrium analysis for heavy metal cation removal using cement kiln dust, Water Sci. Technol., 70 (2014) 1011–1018.

[44] S. Abbaszadeh, S.R. Alwi, C. Webb, N. Ghasemi, I.I. Muhamad, Treatment of lead-contaminated water using activated carbon adsorbent from locally available papaya peel biowaste, J. Clean. Prod., 118 (2016) 210–222.

[45] M. Iqbal, A. Saeed, S.I. Zafar, FTIR spectrophotometry, kinetics and adsorption isotherms modeling, ion exchange, and EDX analysis for understanding the mechanism of Cd^{2+} and Pb^{2+} removal by mango peel waste, J. Hazard. Mater., 164 (2009) 161–171.

[46] M. Uchimiya, I.M. Lima, K.T. Klasson, S. Chang, L.H. Wartelle, J.E. Rodgers, Immobilization of heavy metal ions (CuII, CdII, NiII, PbII) by broiler litter-derived biochars in water and soil, J. Agric. Food Chem., 58 (2010) 5538–5544.

[47] H.N. Trana, S. Youb, H. Chaob, Thermodynamic parameters of cadmium adsorption onto orange peel calculated from various methods: A comparison study, JECE, 4 (2016) 2671–2682.